Results in Physics 19 (2020) 103632

Contents lists available at ScienceDirect

Results in Physics

journal homepage: www.elsevier.com/locate/rinp

Theoretical investigation of thermal disorder in CuCo alloys

Pham Thi Minh Hanh [a], Nguyen Ba Duc [b,*], Nguyen Van Nghia [c], Nguyen Viet Tuyen [d,e,*], Ho Khac Hieu [d,e,*]

[a] Hanoi Pedagogical University No2, Nguyen Van Linh, Vinh Phuc 15900, Viet Nam
[b] Tan Trao University, Km 6, Yen Son, Tuyen Quang 301910, Viet Nam
[c] Faculty of Electrical and Electronics Engineering, Thuyloi University, 175 Tay Son, Dong Da, Ha Noi 116705, Viet Nam
[d] Institute of Research and Development, Duy Tan University, 03 Quang Trung, Hai Chau, Da Nang 550000, Viet Nam
[e] The Faculty of Natural Sciences, Duy Tan University, 03 Quang Trung, Hai Chau, Da Nang 550000, Viet Nam

ARTICLE INFO

Keywords:
Thermal disorder
Anharmonicity
CuCo
Einstein model
Debye–Waller factor

ABSTRACT

In this work, we investigate thermal disorder in intermetallic CuCo alloys by extending the anharmonic correlated Einstein model in extended X-ray absorption fine structure (EXAFS) theory. The expressions of bond-stretching force constants, Einstein frequency and temperature, the atomic mean-square relative displacement characterizing the EXAFS Debye–Waller factor have been derived in terms of Morse potential parameters. We perform numerical calculations for CuCo alloys up to temperature 800 K to study the temperature effects on these thermodynamic quantities. Our research shows that Co–Co bonds are stiffer than Cu–Cu bonds. This leads to the atomic mean-square relative displacement curve of CuCo alloys is lower than the one of Cu metal, but higher than the one of bulk Co. The increasing of Co concentration in CuCo alloys will make the increasing of thermal disorder in the alloy system. Moreover, the dynamic disorder caused by thermal lattice vibrations gives significant contribution to the EXAFS Debye–Waller factor at high temperature.

1. Introduction

The binary CuCo alloys recently attract the attention of widespread research community due to their interesting physical properties such as isotropic giant magnetoresistance [1], superparamagnetism [2], spin-glass-like behavior [3], high strength nanocrystalline [4], and the kinetics of growth of nanocrystalline grains [5]. CuCo alloys turn out as an immediate choice for industrial applications because of the relative abundance and low cost of copper and cobalt metals. At ambient conditions, Cu is in face-centered cubic (FCC) structure, while Co is a hexagonal close packed (HCP) metal. By magnetron sputtering CuCo crystalline alloys were observed remaining single FCC phase up to 80% concentration of cobalt metal [6]. Using rapid quenching techniques, Klement reported a single phase FCC solid solution of copper and cobalt in (0–15) and (75–100) at.% Co ranges [7].

Although many studies have been performed to investigate structural evolution [8], magnetic and transport properties [1,2,9] of CuCo alloys, there are only several works regarding to the thermal disorder in the intermetallic CuCo alloys. Indeed studying this fact in detail is a fundamental for developing magneto-caloric applications [10]. The magnetoresistive effect is not only strongly dependent on the size of magnetic particles but also the thermodynamic treatments controlling the microstructural evolution of the alloy. Thermal disorder effect causes the expansion of atomic positions in crystals which leads to a non-Gaussian distribution of interatomic distances [11,12]. Extended X-ray absorption fine structure (EXAFS) is one of the effective methods for the investigation of structure and thermal disorder of crystalline as well as amorphous materials [13,14]. In order to analyze the thermal lattice vibration effects on EXAFS oscillation, the cumulant expansion approach was presented [15]. In this approach, the second cumulant σ^2 corresponds to the parallel mean-square relative displacement (MSRD) of the bond between absorber and backscatterer atoms. It describes the variance of distance distribution function. This parameter affects sensitively on amplitude of EXAFS through the factor $W(k) = \exp(-2\sigma^2 k^2)$ (where k is the wavenumber) [16], and then is so-called the EXAFS Debye–Waller factor (DWF). Theoretically, the EXAFS DWF is defined as

$$\sigma^2 = \left\langle \left[\vec{R}.\left(\vec{u}_i - \vec{u}_0\right) \right]^2 \right\rangle = \left\langle u_i^2 \right\rangle + \left\langle u_0^2 \right\rangle - 2\left\langle u_i u_0 \right\rangle \quad (1)$$

where $\langle u_i^2 \rangle$ and $\langle u_0^2 \rangle$ are uncorrelated mean square displacement (MSD) of the *zero*th and the *i*th atoms, respectively; the term $2\langle u_i u_0 \rangle$ is the parallel displacement correlation function (DCF); and $\vec{u}_0$ and $\vec{u}_i$ are the atomic displacements of the *zero*th and the *i*th sites from their

* Corresponding authors.
E-mail addresses: ducnb@daihoctantrao.edu.vn (N.B. Duc), nguyenviettuyen@hus.edu.vn (N.V. Tuyen), hieuhk@duytan.edu.vn (H.K. Hieu).

https://doi.org/10.1016/j.rinp.2020.103632
Received 13 September 2020; Received in revised form 11 November 2020; Accepted 15 November 2020
Available online 19 November 2020

equilibrium positions; $\vec{R}$ is the unit vector at the *zero*th site pointing towards the *i*th site, and the brackets stand for the ensemble averaging.

In present work, we investigate the thermodynamic properties of CuCo alloys based on the anharmonic correlated Einstein model (ACEM) [17] in EXAFS theory. We assume that intermetallic CuCo alloys remain stable in FCC structure with any cobalt composition. Main aim of the present work is to develop the ACEM for binary alloys to derive the interatomic effective potential, bond-stretching force constants, Einstein frequency and temperature, and parallel MSRD characterizing for EXAFS DWF. The temperature effects on Einstein frequency and temperature, EXAFS DWF and related thermodynamic quantities are considered by performing numerical calculations for CuCo alloys up to temperature of 800 K which is below the melting temperatures of Cu and Co metals [18,19] using the pair interaction Morse potential.

2. Theoretical approach

2.1. Anharmonic correlated Einstein model

Firstly, we make a brief report of the ACEM [17] and its application for FCC and HCP structures. This model is the extension of the correlated Einstein model in order to include the anharmonicity contributions to EXAFS cumulants. In this model, a local vibration picture of absorber and back-scatterer is considered. The author proposed an anharmonic interatomic effective potential V_{eff} that includes the interactions between absorbing and back-scattering atoms and their nearest-neighbors. Because of the asymmetry of the potential, the effective potential V_{eff} is expressed as a function of the thermal expansion $x = r - r_0$ along the bond direction as

$$V_{eff}(x) = \varphi(x) + \sum_{j\neq i} \varphi\left(\frac{\mu}{M_i} x \hat{R}_{AB}\hat{R}_{ij}\right); \quad \mu = \frac{M_A M_B}{M_A + M_B} \approx \frac{1}{2}k^0_{eff}x^2 + k^0_3 x^3 + \cdots \tag{2}$$

where r and r_0 are, respectively, the instantaneous and equilibrium bond length between absorbing and back-scattering atoms; $\varphi(x)$ describes the interaction between absorber and backscatterer. The influence of the neighboring atoms to the oscillation of absorber and back-scatterer is characterized by term $\sum_{j\neq i}\varphi\left(\frac{\mu}{M_i}x\hat{R}_{AB}\hat{R}_{ij}\right)$, where the sum i is over absorber ($i = A$) and back-scatterer ($i = B$), and the sum j is over all their nearest-neighbor atoms, excluding the absorber and back-scatterer themselves; masses of the absorbing and back-scattering atoms are denoted by M_A and M_B, correspondingly; k^0_{eff} and k^0_3 are, respectively, the effective and cubic bond-stretching force constants caused by an asymmetry in the pair distribution function because of thermal disorder.

Originally, the ACEM was developed for pure crystalline materials [17]. For FCC and HCP crystals, each atom is bonded to twelve nearest-neighbor atoms. Applying the ACEM for these systems, there are twenty-two pair interactions between absorbing and back-scattering atoms with their nearest-neighbor sites, except for the absorber and back-scatterer themselves. The anharmonic effective potential $V_{eff}(x)$ for FCC and HCP crystals can be clearly re-written as

$$V_{eff}(x) = \varphi(x) + 2\varphi\left(-\frac{x}{2}\right) + 8\varphi\left(-\frac{x}{4}\right) + 8\varphi\left(\frac{x}{4}\right). \tag{3}$$

Let us assume that the interaction $\varphi(r)$ between atoms in the system can be described by the Morse potential function as follows

$$\varphi(r) = D\left\{\exp\left[-2\alpha(r-r_0)\right] - 2\exp\left[-\alpha(r-r_0)\right]\right\}, \tag{4}$$

where r_0 is the nearest-neighbor distance in the equilibrium reference structure, D is the dissociation energy and α describes the width of the pair potential. This simple pairwise potential function has been extensively used because of its many advantages. For example, it accounts for the anharmonicity of real bonds, and it also includes the effects of bond breaking.

By making the Taylor expansion of this potential up to the third order of the deviation of instantaneous bond length $x = r - r_0$, we have

$$\varphi(x) \approx D\left(-1 + \alpha^2x^2 - \alpha^3x^3\right). \tag{5}$$

Substituting Eq. (5) into Eq. (3) we obtain the force constants of FCC and HCP crystals in terms of Morse potential parameters as follows

$$k^0_{eff} = 5D\alpha^2; \quad k^0_3 = -\frac{3}{4}D\alpha^3. \tag{6}$$

2.2. Thermodynamic properties of AB alloys

Let us consider substitutional AB alloys in which A atoms composing the metallic A crystal are substituted by B atoms. The Morse potential parameters D_{AB} and α_{AB} for A–B interactions can be derived approximately as

$$D_{AB} = \frac{1}{2}\left(D_A + D_B\right); \alpha^2_{AB} = \frac{D_A\alpha^2_A + D_B\alpha^2_B}{D_A + D_B}. \tag{7}$$

Denoting the concentration of A and B in A–B alloys, respectively, by X_A and X_B, we have $0 \le X_A, X_B \le 1$ and $X_A + X_B = 1$. For the simplicity of building the model, we assume $X_A \ge X_B$. Due to the fact that the interatomic effective potential V_{eff} of A–B alloys is contributed by both A–B and A–A pairs, we estimate the potential V_{eff} roughly as

$$V_{eff} = 2X_BV^{AB}_{eff} + (X_A - X_B)V^A_{eff}, \tag{8}$$

where V^{AB}_{eff} and V^A_{eff} are, correspondingly, the effective potential between A and B atoms, and between A atoms.

From Eqs. (2) & (8), we derive the bond-stretching force constants k_{eff} and k_3 of AB alloy as

$$k_{eff} = 2X_Bk^{AB}_{eff} + (X_A - X_B)k^A_{eff}, \quad k_3 = 2X_Bk^{AB}_3 + (X_A - X_B)k^A_3, \tag{9}$$

where k^A_{eff} and k^A_3 are the force constants derived for FCC A crystal as

$$k^A_{eff} = 5D_A\alpha^2_A; \quad k^A_3 = -\frac{3}{4}D_A\alpha^3_A, \tag{10}$$

and k^{AB}_{eff} and k^{AB}_3 are derived from the interatomic effective potential V^{AB}_{eff} between A and B atoms

$$k^{AB}_{eff} = \left[1 + 8(\mu^2_A + \mu^2_B)\right]D_{AB}\alpha^2_{AB}; \quad k^{AB}_3 = -\left[1 - \mu^3_A - \mu^3_B\right]D_{AB}\alpha^3_{AB}, \tag{11}$$

with

$$\mu_A = \frac{M_A}{M_A + M_B}, \quad \mu_B = \frac{M_B}{M_A + M_B}. \tag{12}$$

The Einstein frequency and Einstein temperature of alloy system can be obtained, respectively, as [17]

$$\omega_E = \sqrt{\frac{k_{eff}}{\mu}} \quad ; \quad \theta_E = \frac{\hbar\omega_E}{k_B}, \tag{13}$$

where μ is the reduced mass in ACEM model

$$\mu = 2X_B\mu_{AB} + (X_A - X_B)\mu_{AA}, \tag{14}$$

and $\mu_{AB} = \frac{M_AM_B}{M_A + M_B}$, $\mu_{AA} = \frac{M_A}{2}$.

And the second EXAFS cumulant of AB alloy in ACEM [17] is derived as

$$\sigma^2 = \left\langle (x - \langle x\rangle)^2\right\rangle = \frac{\hbar\omega_E}{2k_{eff}}\frac{1+z}{1-z} = \sigma^{(2)}_0\frac{1+z}{1-z}, \tag{15}$$

where $z = \exp(-\hbar\omega_E/k_BT)$, k_B is the Boltzmann constant and $\sigma^{(2)}_0 = \frac{\hbar\omega_E}{2k_{eff}}$ is the zero-point contribution to the second cumulant.

Table 1
The Morse potential parameters of Cu–Cu, Co–Co and Cu–Co interactions.

Bond	D (Å)	α (eV)	r_0 (Å^{-1})	Ref.
Cu–Cu	0.3429	1.3588	2.8660	[20]
Co–Co	0.4200	1.3800	2.8000	[21]
Cu–Co	0.3814	1.3705	2.8330	Calculated

Table 2
The bond-stretching force constants k_{eff}, k_3, Einstein frequency ω_E and Einstein temperature θ_E, and zero-point contribution σ_0^2 to the EXAFS DWF derived from developed ACEM.

		k_{eff} (eV/Å^2)	ω_E (×10^{13} Hz)	θ_E (K)	σ_0^2 (×10^{-4} Å^2)
Cu	Present	3.166	3.10	237.05	32.29
	Exp. [22]	3.12 ± 0.06	–	233	36 ± 2
$Cu_{90}Co_{10}$	Present	3.25	3.16	241.10	31.99
	Exp. [22]	3.81 ± 0.06	–	269	32 ± 1
$Cu_{80}Co_{20}$	Present	3.33	3.21	245.13	31.71
	Exp.	–	–	–	–
$Cu_{70}Co_{30}$	Present	3.42	3.26	249.16	31.44
	Exp.	–	–	–	–
$Cu_{60}Co_{40}$	Present	3.50	3.31	253.19	31.18
	Exp.	–	–	–	–
$Cu_{50}Co_{50}$	Present	3.59	3.37	257.21	30.93
	Exp.	–	–	–	–
$Cu_{40}Co_{60}$	Present	3.67	3.42	261.24	30.69
	Exp.	–	–	–	–
$Cu_{30}Co_{70}$	Present	3.75	3.47	265.27	30.47
	Exp.	–	–	–	–
$Cu_{20}Co_{80}$	Present	3.84	3.52	269.30	30.25
	Exp.	–	–	–	–
$Cu_{10}Co_{90}$	Present	3.92	3.58	273.33	30.05
	Exp.	–	–	–	–
Co	Present	3.999	3.62	276.68	29.84
	Exp. [22]	4.31 ± 0.06	–	285	30 ± 1

3. Numerical calculations and discussion

In this section, numerical calculations are performed for CuCo alloys with various concentrations of Co element. The Morse potential parameters of Cu–Cu, Co–Co and Cu–Co interactions are shown in Table 1. [20,21]

Applying the developed ACEM, the force constants, the Einstein frequency and temperature of Cu, Co metals and CuCo alloys are derived. We list these calculated thermodynamic quantities in the Table 2. As we can observe from this table, the values of Einstein temperature of Cu, Co metals and CuCo alloys in our calculations are reasonably consistent with the ones derived from the fitting Einstein model with EXAFS measurements [22]. The difference between our calculated result and the measured one of Einstein temperature is about 2%–3% for metals and about 10% for $Cu_{90}Co_{10}$ alloy. Here it should be noted that the Einstein temperature is a significant physical quantity derived in within view of the Einstein model. It could be seen as a rough threshold temperature so that at a higher temperature, classical considerations for thermodynamic properties of solids can be applicable. The Einstein temperature of Co metal is higher than one of Cu. This is due to the smaller effective force constant k_{eff} obtained for Cu metal in comparison with bulk Co as we can see from Eq. (12). It reflects the fact that Cu–Cu bonds are softer than Co–Co bonds. It causes a phenomenon that Cu lattice shows a greater thermal disorder. As we can see in the following, the greater thermal disorder in Cu system is equivalent to the higher parallel MSRD of bulk Cu comparing to Co metal.

Using the calculated effective force constants k_{eff} and Einstein temperatures ω_E, we derive the values of second cumulants of Cu and Co metals at functions of temperature. In Figs. 1 & 2, we present our theoretical calculations along with experimental measurements of

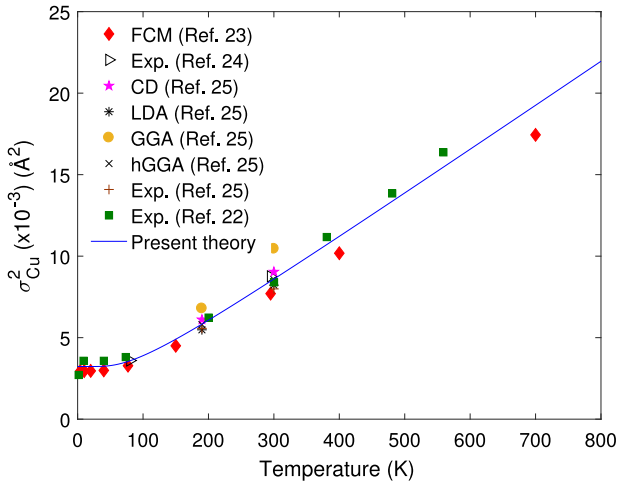

Fig. 1. (Color online) Temperature dependence of the second cumulant of Cu metal. Previous experimental measurements and theoretical calculations are shown for comparison [22–25].

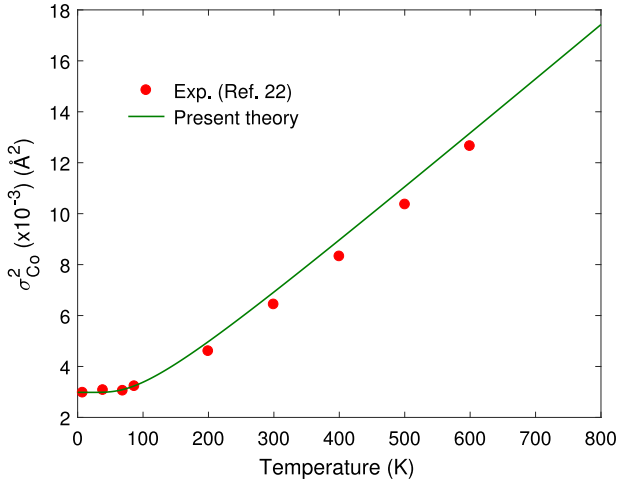

Fig. 2. (Color online) Temperature dependence of the second cumulant of Co metal. Experimental measurements are shown for comparison [22].

MSRDs of Cu and Co metals, respectively, up to temperature 800 K. As it can be seen from these two figures, the DWFs derived from ACEM are in good agreement with available experimental measurements and theoretical calculations for both Cu and Co metals [22–25]. It confirms the ACEM is reliable and applicable to investigate the temperature-dependent EXAFS DWF of metals. We can realize that the DWF is an increasing function of temperature, and above 150 K, it is the almost linear proportion to temperature. The slopes of DWF curves $d\sigma^2/dT$ in temperature region beyond 150 K of Cu and Co metals are, respectively, 2.62×10^{-5} Å^2/K and 2.05×10^{-5} Å^2/K. The rapid increasing of DWF function shows the significant contributions of thermal disorder at high temperature.

The temperature dependence of second cumulants of CuCo alloys with various Co concentration is shown in Fig. 3. As we can see from this figure, the parallel MSRD of CuCo alloys increases with the increasing of Co concentration. This effect can be explained as follows: When Cu atoms are substituted by Co atoms in the Cu matrix, the dispersed Co atoms will be bound to Cu atoms with stiffer bonds compared to Cu–Cu interactions. As a result, CuCo alloys show a weaker thermal disorder (corresponding to lower DWF) comparing to Cu metals. Numerically, the theoretical slopes of DWF curves $d\sigma^2/dT$ in temperature region beyond 200 K of $Cu_{90}Co_{10}$, $Cu_{50}Co_{50}$ and $Cu_{10}Co_{90}$ alloys are

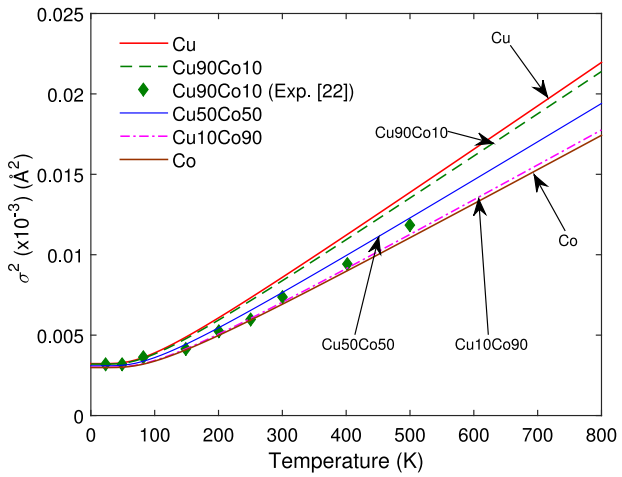

Fig. 3. (Color online) Temperature dependence of the second cumulant of CuCo alloys with various Co concentration. Experimental measurements are shown for comparison [22].

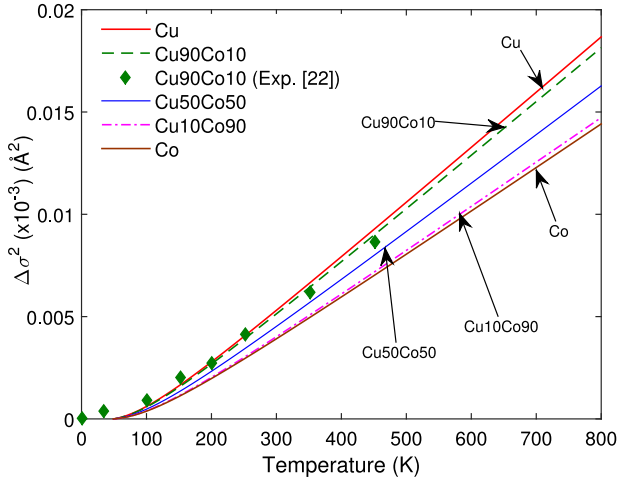

Fig. 4. (Color online) The change of second cumulant of CuCo alloys relative to the reference at temperature of 50 K. Experimental measurements are shown for comparison [22].

predicted, respectively, as 2.55×10^{-5} Å^2/K, 2.30×10^{-5} Å^2/K and 2.09×10^{-5} Å^2/K. Moreover, our EXAFS DWF results of $Cu_{90}Co_{10}$ (dashed line) overestimate the experimental EXAFS measurements by Cezar et al. [22] (closed diamond symbols). This phenomenon originates from the nature of EXAFS DWF as explained in the next paragraph.

It is worth to mentioning that the second cumulant σ^2 corresponds to the parallel atomic MSRD characterizing the EXAFS Debye–Waller factor. It includes both the static disorder and thermal disorder. The first contribution is so-called structural disorder which is caused by strain or alloying. Meanwhile, the thermal disorder is dynamic disorder originated from the thermal lattice vibrations. It provides information of bond-stretching force constants between pair absorber–backscatterer atoms which correspond to the dynamical properties of them [26]. For this reason, if we calculate the change of EXAFS DWF relative to the one at a reference temperature, we can eliminate errors in calculation of the static disorder. In Fig. 4, we show the relative change of the EXAFS DWF to the reference at temperature of 50 K denoted by $\Delta\sigma^2$ (in 10^{-3} Å^{-2}). As observed from this figure, after removing the structural disorder, our theoretical prediction of EXAFS DWF change of $Cu_{90}Co_{10}$ alloy is in good agreement with measurement of Cezar et al. [22] (closed diamond symbols).

Before making conclusions, it should be noted that from the definition of EXAFS DWF in Eq. (1), the values of EXAFS DWFs are dependent on the MSDs of central atom, its neighboring atoms and their DCF. It means that the values of EXAFS DWFs depend on the specific local chemical order. Therefore, theoretically, we are able to differentiate between ideal substitutional solid solution and solid solution with an explicit local chemical order based on temperature trends of EXAFS DWFs.

4. Conclusions

We have investigated thermodynamic properties of CuCo alloys based on the developed anharmonic correlated Einstein model. Using the Morse potential, numerical calculations have been performed to derive the bond-stretching force constants, Einstein frequency and temperature and mean-square relative displacement of CuCo alloys up to temperature 800 K with various Co concentration. Our research shows that Co–Co bonds are stiffer than Cu–Cu bonds. This leads to the weaker thermal disorder in CuCo alloys in comparison to Cu metal. Furthermore, the dynamic disorder due to thermal lattice vibrations is significant to the EXAFS DWF at high temperature. The reasonable agreement between our theoretical prediction and previous measurements shows that the developed ACEM is applicable to investigate thermodynamic properties of alloys in EXAFS theory. The reported results increase the database of the Einstein frequency and corresponding temperature, and the mean-square relative displacement of CuCo alloys. These data can be used to verify future EXAFS experiments.

CRediT authorship contribution statement

Pham Thi Minh Hanh: Data curation, Formal analysis, Investigation, Methodology, Writing - original draft, Writing - review & editing. **Nguyen Ba Duc:** Resources, Project administration, Funding acquisition, Supervision, Investigation, Writing - original draft, Writing - review & editing. **Nguyen Van Nghia:** Validation, Writing - review & editing. **Nguyen Viet Tuyen:** Validation, Visualization, Writing - review & editing. **Ho Khac Hieu:** Conceptualization, Resources, Validation, Writing - original draft, Writing - review & editing.

Declaration of competing interest

The authors declare that they have no known competing financial interests or personal relationships that could have appeared to influence the work reported in this paper.

Acknowledgments

The authors would like to acknowledge Prof. Nguyen Van Hung for useful comments and suggestions. This research is funded by the Vietnam National Foundation for Science and Technology Development (NAFOSTED) under grant number 103.01–2019.55.

References

[1] Berkowitz AE, Mitchell JR, Carey MJ, Young AP, Zhang S, Spada FE, et al. Giant magnetoresistance in heterogeneous Cu–Co alloys. Phys Rev Lett 1992;68:3745–8.
[2] Hickey BJ, Howson MA, Musa SO, Wiser N. Giant magnetoresistance for superparamagnetic particles: Melt-spun granular CuCo. Phys Rev B 1995;51:667–9.
[3] Idzikowski B, Rößler UK, Eckert D, Nenkov K, Müller K-H. Spin-glass–like ordering in giant magnetoresistive CuCo. Europhys Lett (EPL) 1999;45(6):714–20.
[4] Bachmaier Andrea, Rathmayr Georg Benedikt, Schmauch Jörg, Schel Norbert, Stark Andreas, de Jong Niels, et al. High strength nanocrystalline Cu–Co alloys with high tensile ductility. J Mater Res 2019;34(1):58–68.
[5] Cezar Júlio C, Tolentino Hélio CN, Knobel Marcelo. Structural, magnetic, and transport properties of Co nanoparticles within a Cu matrix. Phys Rev B 2003;68:054404.

[6] Childress JR, Chien CL. Reentrant magnetic behavior in fcc Co–Cu alloys. Phys Rev B 1991;43:8089–93.
[7] Klement Jr W. Solid solutions in gold-cobalt and copper-cobalt alloys 227. 1963, p. 965–70.
[8] Bonetti E, Pasquini L, Sampaolesi E, Savini L. Structural evolution of a Cu1–xCox alloy during thermal heating studied by acoustic spectroscopy. J Non-Crystal Solids 1998;232–234:239–44.
[9] Wecker J, von Helmolt R, Schultz L, Samwer K. Giant magnetoresistance in melt spun CuCo alloys. Appl Phys Lett 1993;62(16):1985–7.
[10] Sagotra Arun K, Errandonea Daniel, Cazorla Claudio. Mechanocaloric effects in superionic thin films from atomistic simulations. Nature Commun 2017;8(1):963.
[11] Dalba G, Fornasini P. EXAFS Debye–Waller Factor and thermal vibrations of crystals. J Synchrotron Radiat 1997;4(4):243–55.
[12] Momozawa Ai, Telle Rainer. X-ray diffraction study of TiB_2, $W2B_4$, and CrB_2 at high temperatures. Vacuum 2018.
[13] Kousa M, Iwasaki S, Ishimatsu N, Kawamura N, Nomura R, Kakizawa S, et al. Element-selective elastic properties of $Fe_{65}Ni_{35}$ invar alloy and $Fe_{72}Pt_{28}$ alloy studied by extended X-ray absorption fine structure. High Press Res 2020;40(1):130–9.
[14] Popov VV, Menushenkov AP, Ivanov AA, Yastrebtsev AA, Gaynanov BR, d'Acapitoo F, et al. A XAFS investigation of amorphous-to-crystalline and fluorite-to-pyrochlore phase transitions in $Ln_2M_2O_7$ (Ln=Gd, Tb, Dy; M=Ti, Zr). Radiat Phys Chem 2020;175:108469, 7th International Conference on X-ray Absorption Fine Structure – XAFS2018.
[15] Bunker Grant. Application of the ratio method of EXAFS analysis to disordered systems. Nucl Instrum Methods Phys Res 1983;207(3):437–44.
[16] Crozier ED, Rehr JJ, Ingalls R. In: Koningsberger DC, Prins R, editors. X-ray absorption: Principles, applications, techniques of EXAFS, SEXAFS and XANES. 1st ed. Wiley-Interscience; 1988.
[17] Hung Nguyen Van, Rehr JJ. Anharmonic correlated Einstein-model Debye–Waller factors. Phys Rev B 1997;56:43–6.
[18] Errandonea Daniel. The melting curve of ten metals up to 12 GPa and 1600 K. J Appl Phys 2010;108(3):033517.
[19] Errandonea Daniel, Schwager Beate, Ditz Reiner, Gessmann Christine, Boehler Reinhard, Ross Marvin. Systematics of transition-metal melting. Phys Rev B 2001;63:132104.
[20] Girifalco LA, Weizer VG. Application of the morse potential function to cubic metals. Phys Rev 1959;114:687–90.
[21] Lindroos M, Barnes CJ, Hu P, King DA. The termination and multilayer relaxation at the Co{1010} surface. Chem Phys Lett 1990;173(1):92–6.
[22] Cezar JC, Abreu NP, Tolentino HCN. Debye–Waller factor study of Co, Cu and CoCu granular alloy. Phys Scr 2005;418.
[23] Sevillano E, Meuth H, Rehr JJ. Extended X-ray absorption fine structure Debye–Waller factors. I. Monatomic crystals. Phys Rev B 1979;20:4908–11.
[24] Yokoyama Toshihiko, Satsukawa Tomiaki, Ohta Toshiaki. Anharmonic interatomic potentials of metals and metal bromides determined by EXAFS. Japan J Appl Phys 1989;28(Part 1, No. 10):1905–8.
[25] Vila Fernando D, Rehr JJ, Rossner HH, Krappe HJ. Theoretical X-ray absorption Debye–Waller factors. Phys Rev B 2007;76:014301.
[26] Hong NT, Hieu HK, Duc NB, Phuong DD, Tuyen NV, Khoa DQ. Anharmonic correlated Debye model for thermal disorder in iron-rich B2-FeAl intermetallic alloy. Vacuum 2019;163:210–5.